

9688

NACA TN 2509

TECH LIBRARY KAFB, NM  
0065511

# NATIONAL ADVISORY COMMITTEE FOR AERONAUTICS

TECHNICAL NOTE 2509

A SELF-SYNCHRONIZING STROBOSCOPIC SCHLIEREN SYSTEM  
FOR THE STUDY OF UNSTEADY AIR FLOWS

By Leslie F. Lawrence, Stanley F. Schmidt,  
and Floyd W. Looschen

Ames Aeronautical Laboratory  
Moffett Field, Calif.



Washington

October 1951

AFMDC  
TECHNICAL LIBRARY  
AFL 2811

*10-28-51*



0065511

1

## NATIONAL ADVISORY COMMITTEE FOR AERONAUTICS

## TECHNICAL NOTE 2509

## A SELF-SYNCHRONIZING STROBOSCOPIC SCHLIEREN SYSTEM

## FOR THE STUDY OF UNSTEADY AIR FLOWS

By Leslie F. Lawrence, Stanley F. Schmidt,  
and Floyd W. Looschen

## SUMMARY

A self-synchronizing stroboscopic schlieren system developed for the visualization of unsteady air flows about aerodynamic bodies in wind tunnels is described. This instrument consists essentially of a conventional stroboscopic schlieren system modified by the addition of electronic and optical elements to permit the detailed examination of phenomena of cyclic nature, but of fluctuating frequency. An additional feature of the device makes possible the simulation of continuous slow motion, at arbitrarily chosen rates, of particular flow features.

Physically, the instrument is a schlieren system having two light paths with displaced light sources and focal points but using common primary reflectors. One of these light paths, utilizing a steady light source, is intercepted by a phototube, which receives signals in the form of changes of light intensity corresponding to fluctuations of the air-stream density. The output of this phototube in turn triggers a stroboscopic light source, thereby producing a stationary image of an oscillating disturbance in the other light path. Simulated slow motion is obtained electronically by causing the flash of the stroboscopic light to lag the synchronizing signal from the phototube by a constantly increasing increment of time.

Circuit descriptions and an itemized list of the components used are presented.

## INTRODUCTION

The fundamental study of such aerodynamic phenomena as shock-wave boundary-layer interaction, development of vortices in a Kármán vortex street, and pulsating flows in air-induction systems often makes desirable the detailed optical examination of oscillating air flows about wind-tunnel models. This examination is commonly accomplished by means of stroboscopic schlieren equipment. It is invariably discovered, however, that the small variations in velocity to which subsonic wind-tunnel flows are subject are reflected as variations in the frequency of the disturbance under investigation. Furthermore, in many instances the

PERMANENT  
RECORD

frequency of the phenomenon proves inconstant. The frequency variations from these two sources are often sufficiently erratic that no visual continuity can be obtained with conventional stroboscopic equipment.

To satisfy the need for an instrument permitting the visualization of fluctuating-frequency flows, the development of a self-synchronizing stroboscopic schlieren system was undertaken. The essential requirement was that the stroboscopic frequency be controlled by, and be in synchronism with, the particular flow irregularity of interest in the investigation. Additional desirable features were a method to effect slow motion of the image of the disturbance through its cycle during visual observation, and a method for metering the average frequency of the disturbance. The instrument was to be capable of dealing with phenomena having frequencies as high as 10,000 cycles per second.

This paper describes the self-synchronizing stroboscopic schlieren instrument developed to satisfy these requirements and certain limitations controlling the effective application of the instrument. Selected photographs are presented to provide typical illustrations of the flow detail visible to an observer, and of the flexibility of the instrument.

#### DESCRIPTION

A perspective view and a block diagram of the instrument are given in figures 1 and 2, respectively. The instrument consists essentially of a dual schlieren system and associated electronic controls.

The primary schlieren system utilizes a constant-intensity light source. Variations of the light intensity in a selected portion of the viewing field of this system are used to control the flashing of the light source of a secondary schlieren system. By appropriate selection of the size and position of the controlling portion of the primary field, the flashing of the secondary light source can be made to coincide with the instants at which successive occurrences of the phenomenon being studied have reached a fixed geometrical position. It can be seen that the over-all result is to produce a stroboscopic effect which is independent of the regularity of the phenomenon being studied.

A cyclic presentation of the growth and motion of the phenomenon is obtained by controlled delay of the flashing of the stroboscopic light source. Each successive control signal received from the fluctuating light in the primary viewing field is delayed by a constantly increasing interval. The effect of the constantly increasing delay is to present images on the viewing screen of the secondary schlieren which show the disturbance at different phases of its development. The combined effect of many images is to produce an illusion of viewing the development of the disturbance in slow motion.

### Optical Equipment

The two schlieren systems have separate light sources, images, knife-edge positions, and focusing planes, but they utilize the same primary reflectors.

The method by which the primary system detects disturbances and actuates the stroboscopic system may be seen from an inspection of the light paths shown in figure 2. Light rays from the primary source (1) are collimated by the first reflector (2), traverse the wind-tunnel test section, and are then focused by the second reflector (3) at the knife edge (4). A small plane mirror (5) inserted in the plane of the image formed at (6) directs a light beam to the phototube (7). This mirror is placed in the area traversed by the image of the fluctuating disturbance being investigated (e.g., a moving shock wave). The knife edge (4) is adjusted to maximize the variation of light intensity impinging on the phototube. The phototube responds to the fluctuating light intensity and produces an electrical signal which is used to control the flashing of the light source of the secondary stroboscopic schlieren system.

The optimum size of mirror (5) is determined by the size of the particular object being examined. For the applications described, repetitive flashes at identical points in the cycle were obtained with a 1/64-inch-diameter mirror in an image field of 2-inches diameter.

### Electronic Components

A block diagram of the electronic equipment through which the current generated by the phototube controls the flashing of the light source for the stroboscopic schlieren system is also illustrated in figure 2. This equipment also indicates the average frequency of the disturbance and provides the simulated slow motion of the cyclic phenomenon on the secondary viewing screen.

A schematic representation of the voltage output as a function of time for the various blocks is presented in figure 3.<sup>1</sup>

The output of the phototube is passed first through the filter (fig. 2, block 8) to remove all signals of frequency greater than some predetermined amount, which in this case is 10,000 cycles per second. The output of the filter (fig. 3(a)) is amplified (fig. 2, block 9) and sent to a frequency indicator (fig. 2, block 10) where the arithmetical average frequency is indicated. The frequency indicating circuit also

---

<sup>1</sup>For simplicity the wave forms of figure 3 are idealized and not intended to be accurate reproductions.

changes the wave form of the amplified phototube electrical signal to a short electrical pulse (fig. 3(b)), one pulse being generated for each cycle of input. This pulse is sent to the frequency limiting circuit (fig. 2, block 11) which allows the passage of a maximum of approximately 300 electrical pulses per second. The function of this circuit is to provide a maximum limit on the power applied to the mercury lamp, and for disturbance frequencies above 500 cycles per second it allows a relatively constant average power flow to the secondary mercury lamp. The output of the frequency limiting circuit (fig. 3(c)) is sent to the differentiating and amplifying circuit (fig. 2, block 12) which converts the rectangular wave form to short pulses (fig. 3(d)), the maximum frequency of which is now 300 cycles per second. The amplified pulse then triggers the variable time-delay circuit (fig. 2, block 13).

The variable time-delay circuit is essentially a triggered trapezoidal wave generator in which the duration of the generated wave is proportional to and controlled by a voltage (fig. 3(e)) which increases linearly with time. Since the pulses that control the flashing of the secondary light source are derived from the trailing edge of the trapezoidal wave (fig. 3(f)), each light pulse will lag the preceding one by a constant increment of time - thus permitting the cyclic motion of the aerodynamic phenomenon to be visualized in slow motion on the schlieren viewing screen.

The output of the variable time-delay circuit (fig. 3(f)) is coupled to a differentiating and amplifying circuit (fig. 2, block 14) and thereafter amplified by the pulse amplifier (fig. 2, block 15). The output of the pulse amplifier is used to trigger the hydrogen thyatron (fig. 2, block 16) which causes the discharge of a fixed amount of energy (fig. 3(g)) through the secondary, or stroboscopic, light source (fig. 2, block 17). This produces the short flash of light (approximately 5 microseconds duration) which is focused at the secondary knife edge (fig. 2, item 18) and which, according to the position of the plane mirror (fig. 2, item 19) either illuminates the viewing screen of the secondary schlieren system (fig. 2, item 20) or enters the motion-picture camera (fig. 2, item 21).

#### Photographic Records

Photographic records are obtained by diverting the secondary light path into a 35 mm motion-picture camera (see figs. 1 and 2) modified by the deletion of the shutter and the addition of a commutation mechanism (fig. 2, block 22) which is synchronized to interrupt the stroboscopic light during the moving portion of the film cycle. The simulated cyclic-motion feature included in this instrument makes unnecessary a camera of high frame speed to obtain motion pictures of high-frequency disturbances.

## APPLICATIONS AND DISCUSSION

As has been mentioned previously, fluctuations of frequency caused by the small velocity fluctuations occurring in subsonic wind tunnels, as well as those inherent in some aerodynamic phenomena, preclude the use of conventional stroboscopic schlieren systems for measurement of recurrence rates or for detailed examination of high-frequency fluctuating flows. The self-synchronizing stroboscopic schlieren system provides a means for studying such disturbances in the wind tunnel while they occur. An examination of unsteady cyclic disturbances occurring, for example, behind a blunt trailing-edge airfoil permits the observer to study the formation and discharge of vortices from the blunt base. The selected sequence of photographs of figure 4 are presented as an illustration of the detail visible on the viewing screen of such a fluctuating flow. (The fluctuations in this case occur at about 150 cycles per second.) In figure 4(a) the upper vortex has achieved full growth and has just broken away from the rear of the airfoil and a new vortex has begun to form. (Note the rolling up of the boundary layer leaving the upper surface of the airfoil.) The lower vortex is already well developed. In figure 4(b) the new vortex has attained about one-fourth of its ultimate size. Subsequent stages of development are to be seen in figures 4(c), 4(d), and 4(e). Figure 4(f), showing the fully developed vortex following its predecessor downstream, completes the cycle. Figures 5 to 9 are presented as additional illustrations of the application of the instrument. The average frequencies of the fluctuations illustrated by these figures range from 450 cycles per second in the case of the larger cylinder (fig. 5) to 9520 for the flow behind the aerodynamic body seen in figure 9.

In all of these investigations, as well as in that represented by figure 4, it was possible to observe the formation and detachment of the vortices behind the models, and the propagation of pressure waves at any desired rate and for any desired period of time.

These applications of the self-synchronizing stroboscopic schlieren instrument by no means exhaust its possibilities, nor does 10,000 cycles per second represent the maximum frequency range to which it may be adapted. This frequency range was adequate for the particular series of investigations, of which those described in the preceding paragraph are typical examples. Modifications of the electronic circuit, which may be made without great difficulty, would permit use in applications requiring frequencies up to 100,000 cycles per second. Application of the self-synchronizing stroboscopic feature is limited, however, to cyclic phenomena having the following characteristics: (1) The size and shape of each disturbance must be nearly the same, and (2) the time history of each disturbance from a fixed point must be approximately constant for each cycle.

Although the instrument was designed for use in conjunction with a schlieren apparatus to facilitate research investigations of unsteady flow phenomena, the electronic portion may readily be modified for use in any application where a manually controlled stroboscope proves inadequate because of the inconstant frequency of the observed phenomenon. In addition, the variable time-delay feature of the instrument might well be included in numerous other instruments.

Ames Aeronautical Laboratory  
National Advisory Committee for Aeronautics  
Moffett Field, Calif., Aug. 9, 1951

## APPENDIX

## CIRCUIT DESCRIPTION

The schematic diagrams of the electronic circuits are shown in figures 10 and 11 and the components are listed in table I. Inspection of the figures shows that most of the circuits are of conventional design; thus, only the more complex circuits are discussed here.

## Frequency Indicating Circuit

The frequency-indicating circuit is essentially a gas-tube binary scalar modified by the addition of the differentiating circuits (C10, R22 and C11, R25), the rectifying diode (V6), and the frequency-indicating microammeter.

In cases where the signal-to-noise ratio of the amplifier output is low and a precise measurement of frequency is required, the output of the amplifiers is coupled to a synchroscope and a Strobocorr. The synchroscope is used to measure the approximate frequency, and the Strobocorr to obtain the precision necessary. This arrangement is only suitable for frequency ranges from approximately 30 to 4000 cycles per second.

## Frequency-Limiting Circuit

The frequency-limiting circuit is a one-shot multivibrator (V8-1 and V8-2) modified by the addition of tube V7-1. The tube V7-1 is included to insure that capacitor C15 is fully charged during the interval when the grid of V8-1 is beyond cut-off. The duration of the "off" time of V8-2 is initially set at approximately 3300 microseconds by choice of R35 and C15. A pulse derived from the leading edge of the plate signal of V8-2 is used to control succeeding operations.

## Variable Time-Delay Circuit

Variable time delay is achieved by a phantatron time-delay circuit (references 1 and 2) composed of tubes V9 and V10. When the circuit is in the stable quiescent condition, there is no current flow to the plate of V10 due to the bias voltage between grid No. 3 and the cathode. Application of a negative pulse to the cathode of V9-1 causes the plate voltage and consequently the grid No. 1 voltage (via cathode follower V9-2 and capacitor C22) to decrease with respect to ground potential. This decrease of grid No. 1 voltage reduces the total current flowing in V10 and, since R48 is not by-passed, the bias on grid No. 3 decreases with respect to the cathode. A switching action thus takes place so that current flows to the plate circuit. As the charge on C22 leaks off through R50, the plate current increases until a value of plate current is reached for which a further increase in grid No. 1 voltage causes a



decrease in plate current. At this point a switching action takes place, and the current switches from the plate circuit to grids Nos. 2 and 4 of V10, the quiescent condition of the circuit.

The time required for the circuit to return to quiescent condition constitutes the time delay of the circuit. This time is determined by the initial charge on C22. Since C22 is charged through the cathode of V9-2 and the control grid of V10, the initial charge on C22 can be controlled by controlling the quiescent-plate voltage of V10. A saw-toothed voltage from a relaxation-type generator is placed on the cathode of V9-1 through isolating resistor R43. This saw-toothed voltage causes a similar variation in the quiescent plate voltage of V10, and consequently in the quiescent charge on C22, thereby producing a time delay which increases linearly with time. The duration of the saw-toothed wave is very long (2 to 5 sec.) compared to the rate at which the variable-delay circuit receives triggering pulses (approximately 300 per sec.). Thus, even though a jitter of the image on the secondary viewing screen occurs every time the saw-toothed wave recovers, this jitter is not objectionable to the viewer. A switch is provided so that the operator may control the time delay from a manually adjustable potentiometer.

The maximum delay of the variable time-delay circuit must not exceed the minimum interval between pulses as determined by the frequency limiting circuit. Violating this condition results in a variation in the light intensity at the secondary viewing screen which is in synchronism with the saw-toothed wave.

#### The Lamp and Pulsing Circuit

The three-stage pulse amplifier shown in figure 11 produces a 230-volt positive pulse (0.3 microsecond rise time and 1.5 microsecond duration) which drives the grid of a 5C22 hydrogen thyratron (V20). The application of the positive pulse causes the tube to fire, which in turn causes the discharge of the energy stored in capacitors C45 and C46 through V20 and the lamp (an aircooled, high-pressure mercury-arc lamp, type BH-6.) A light flash is emitted which has a duration of approximately 5 microseconds and a peak intensity of 100 times the intensity obtained from the lamp when operated under manufacturer's ratings.

During the interval between pulses, C45 and C46 recharge from the high-voltage power source. The lamp is held conductive by a small direct current (approximately 25 milliamperes) supplied from the high-voltage source via R81. This current performs two functions: First, it eliminates a source of time jitter between the firing of V20 and emission of light from the lamp; second, it allows operation of the lamp at higher

average power dissipation without intermittent misfiring. This results from the fact that the ionization potential of the lamp increases with pressure, which is proportional to average power dissipation. If the pressure increase becomes excessive, reionization of the lamp becomes erratic. By maintaining the lamp in the ionized state, this instability is eliminated.

#### Low-Voltage Control Circuits

Most of the low-voltage switching has been eliminated from the drawings in order to present clearly the essential portions of the circuit. It is sufficient to say that relays and interlocks must be arranged to allow sufficient heating of the filaments of the gas tubes, to protect equipment and personnel, and to provide convenient operation of the equipment.

## REFERENCES

1. Close, R. N., and Lebenbaum, M. T.: Design of Phantatron Time Delay Circuits. Electronics, April 1948, p. 100.
2. Massachusetts Institute of Technology Radar School: Principles of Radar. McGraw-Hill Book Co., Inc., N. Y., 2nd ed. 1946, pp. 2 - 58 through 2 - 64.

TABLE I.— LIST OF COMPONENTS

Resistors

R1	22,000	ohms	1/2W	carbon	R45	68,000	ohms	2W	carbon
R2	22,000	ohms	1/2W	carbon	R46	20,000	ohms	10W	wire
R3	22,000	ohms	1/2W	carbon	R47	6,800	ohms	1W	carbon
R4	22,000	ohms	1/2W	carbon	R48	10,000	ohms	1W	carbon
R5	22,000	ohms	1/2W	carbon	R49	2.2 megohms	1W	carbon	
R6	22,000	ohms	1/2W	carbon	R50	1	megohm	1W	carbon
R7	22,000	ohms	1/2W	carbon	R51	25,000	ohms	5W	carbon
R8	22,000	ohms	1/2W	carbon	R52	10,000	ohms	1W	carbon
R9	22,000	ohms	1/2W	carbon	R53	40,000	ohms	5W	wire
R10	10,000	ohms	1W	carbon	R54	20,000	ohms	5W	wire
R11	470,000	ohms	1W	carbon	R55	270,000	ohms	1W	carbon
R12	680	ohms	1W	carbon	R56	10,000	ohms	1W	carbon
R13	270,000	ohms	1W	carbon	R57	20,000	ohms	5W	wire
R14	1.2	megohms	1W	carbon	R58	40,000	ohms	5W	wire
R15	33,000	ohms	1W	carbon	R59	150	ohms	5W	wire
R16	1	megohm	1W	carbon	R60	47,000	ohms	2W	wire
R17	680	ohms	1W	carbon	R61	70,000	ohms	5W	wire
R18	1,500	ohms	5W	wire	R62	10,000	ohms	25W	Ohmite
R19	100,000	ohms	1W	carbon	R63	50,000	ohms	50W	Ohmite
R20	20,000	ohms	1W	carbon	R64	50,000	ohms	50W	Ohmite
R21	5,000	ohms	5W	wire	R65	100,000	ohms	2W	carbon
R22	3,300	ohms	2W	carbon	R66	2,000	ohms	1W	carbon
R23	100,000	ohms	2W	carbon	R67	2,000	ohms	5W	wire
R24	100,000	ohms	1W	carbon	R68	2,000	ohms	5W	wire
R25	3,300	ohms	2W	carbon	R69	47,000	ohms	1W	carbon
R26	5,000	ohms	5W	wire	R70	10,000	ohms	5W	wire
R27	10,000	ohms	2W	carbon	R71	40,000	ohms	5W	wire
R28	15,000	ohms	5W	wire	R72	5,000	ohms	2W	wire
R29	100,000	ohms	1W	carbon	R73	10,000	ohms	1W	carbon
R30	56,000	ohms	1W	carbon	R74	75	ohms	2W	wire
R31	100,000	ohms	1W	carbon	R75	12,000	ohms	25W	wire
R32	330,000	ohms	1W	carbon	R76	5,000	ohms	10W	wire
R33	20,000	ohms	5W	wire	R77	220,000	ohms	2W	carbon
R34	1,000	ohms	5W	wire	R78	2,500	ohms	10W	wire
R35	2.2	megohms	1W	carbon	R79	75	ohms	10W	wire
R36	10,000	ohms	10W	wire	R80	5	megohms	10W	high volt- age
R37	10,000	ohms	10W	wire	R81	200,000	ohms	400W	wire
R38	10,000	ohms	1W	carbon	R82	10,000	ohms	800W	wire
R39	20,000	ohms	5W	wire	R83	1	megohm	10W	high- voltage
R40	220,000	ohms	1W	carbon	R84	22	ohms	5W	wire
R41	12,500	ohms	5W	wire					
R42	5,600	ohms	1W	carbon					
R43	10,000	ohms	1W	carbon					
R44	5,600	ohms	1W	carbon					

NACA

TABLE I.— CONTINUED

Potentiometers

P1	70,000 ohms	4W wire wound	P5	20,000 ohms	4W wire wound
P2	10,000 ohms	4W wire wound	P6	20,000 ohms	4W wire wound
P3	10,000 ohms	4W wire wound	P7	10,000 ohms	4W wire wound
P4	10,000 ohms	4W wire wound	P8	2 megohms	3W carbon

Inductors

L1	13 henries	40 MA	L8	2.25 microhenries
L2	13 henries	40 MA	L9	2.25 microhenries
L3	8 henries	200 MA	L10	12 henries
L4	8 henries	200 MA	L11	6 henries
L5	.34 henries	Audio Choke	L12	1 millihenry
L6	.34 henries	Audio Choke	L13	1 millihenry
L7	16 millihenries		L14	12 henries

Transformers

T1	117/2.5VCT Filament	T8	117/11,000VCT 200 MA
T2	117/1200 V at 5 MA	T9	GE No. 59G37 high reac-
T3	117/750VCT, 150 MA/5VCT, 3A/6.3VCT, 5A		tance
T4	10,000 ohm primary, interstage	T10	ignition coil
T5	117/6.3VCT Filament	T11	117/5V/5V/5V Filament
T6	117/750VCT, 150MA/5VCT, 3A/6.3VCT, 5A	T12	117/6.3V Filament
T7	117/2.5VCT 10A Filament		

Condensers

C1	.003 mfd	600V paper	C17	.0005 mfd	300V mica
C2	.003 mfd	600V paper	C18	50 mfd	50V electrolytic
C3	10 mfd	25V electrolytic	C19	.001 mfd	600V paper
C4	.1 mfd	600V paper	C20	.001 mfd	600V paper
C5	.1 mfd	600V paper	C21	.5 mfd	600V paper
C6	.1 mfd	600V paper	C22	.005 mfd	600V paper
C7	8 mfd	450V electrolytic	C23	.005 mfd	600V paper
C8	10 mfd	25V electrolytic	C24	.001 mfd	600V paper
C9	12 mfd	450V electrolytic	C25	15 mfd	1500V pyranol
C10	.0005 mfd	300V mica	C26	15 mfd	1500V pyranol
C11	.0005 mfd	300V mica	C27	16 mfd	600V electrolytic
C12	.0005 mfd	300V mica	C28	16 mfd	600V electrolytic
C13	50 mfd	50V electrolytic	C29	8 mfd	600V paper
C14	.5 mfd	600V paper	C30	12 mfd	450V electrolytic
C15	.003 mfd	300V mica	C31	12 mfd	450V electrolytic
C16	16 mfd	450V electrolytic	C32	.0005 mfd	300V mica

TABLE I.— CONCLUDED

Condensers

C33	.01 mfd	600V paper	C43	.002 mfd	600V paper
C34	.5 mfd	600V paper	C44	.1 mfd	600V paper
C35	.05 mfd	600V paper	C45	.04 mfd	12KV oil filled
C36	.05 mfd	600V paper	C46	.04 mfd	12KV oil filled
C37	50 mfd	50V electrolytic	C47	16 mfd	600V electrolytic
C38	.002 mfd	600V paper	C48	16 mfd	600V electrolytic
C39	10 mfd	50V electrolytic	C49	18 mfd	7500V oil filled
C40	.002 mfd	600V paper	C50	.05 mfd	12KV oil filled
C41	10 mfd	50V electrolytic	C51	30 mfd	1500V oil filled
C42	8 mfd	600V electrolytic	C52	4 mfd	600V paper

Tubes

V1	1P21	V14	884
V2	6SJ7	V15	2X2A
V3	6F6G	V16	6H6
V4	884	V17	6AG7
V5	884	V18	807
V6	6H6	V19	807
V7	6SN7	V20	5C22
V8	6SN7	V21	5U4G
V9	6SN7	V22	866/866A
V10	6SA7	V23	866/866A
V11	6SN7	V24	872
V12	5U4G	V25	872
V13	OA3/VR75	V26	872
		V27	872

Miscellaneous

T time-delay relay, 30 seconds  
 D1 dry-disc rectifier  
 Lamp; air cooled, Mercury arc type BH-6



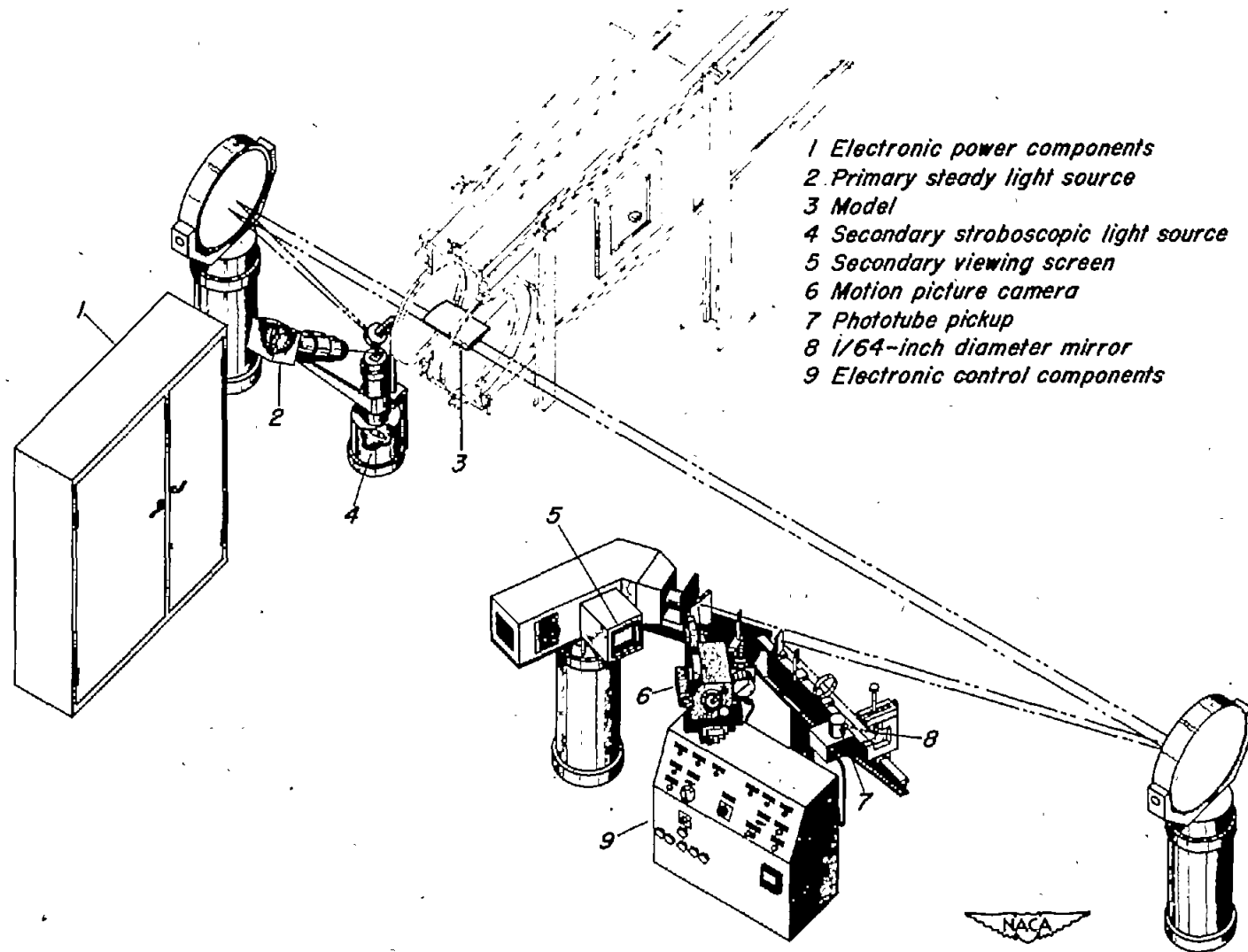


Figure 1.- Perspective view of the self-synchronizing stroboscopic apparatus.



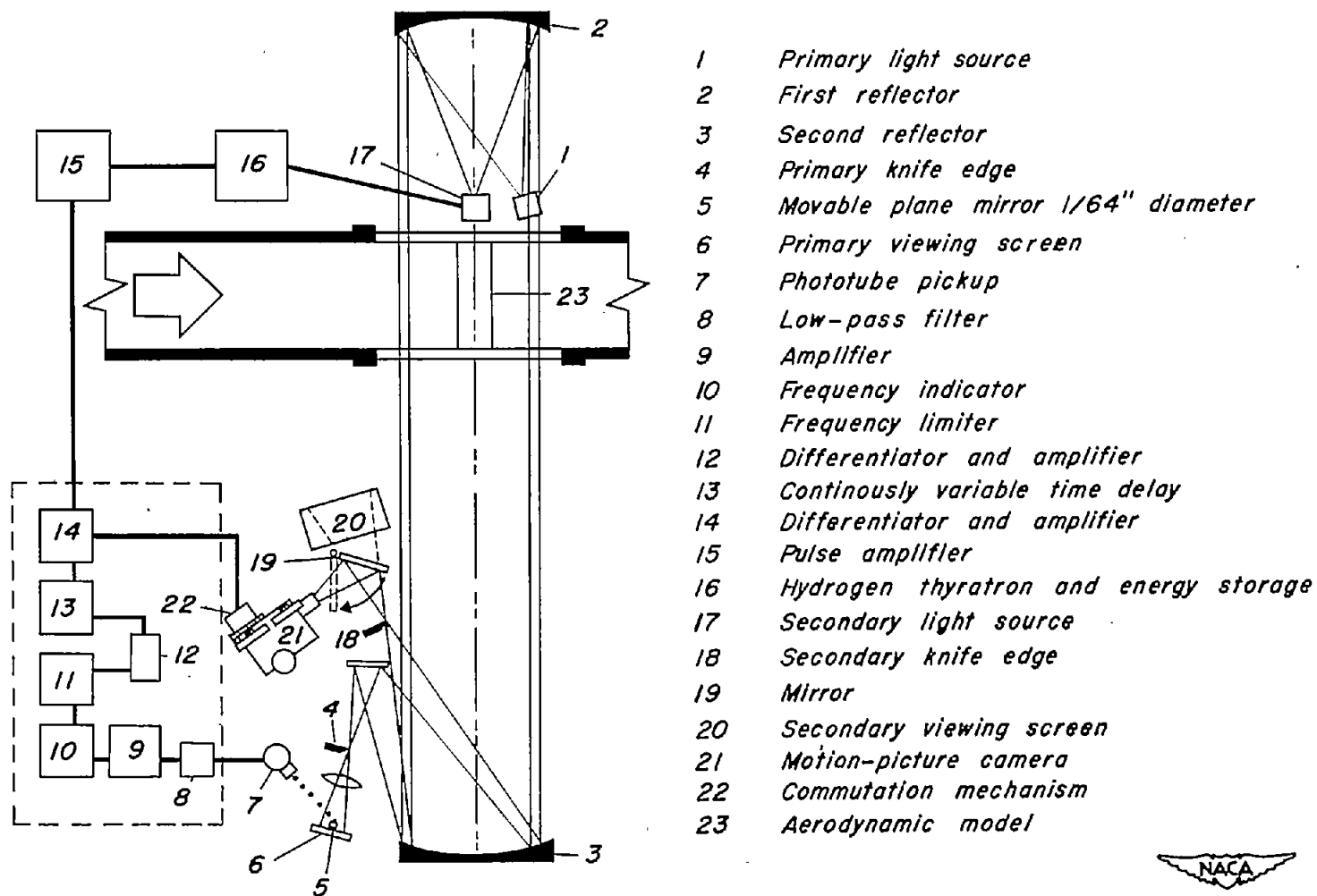


Figure 2.- Block diagram of the self-synchronizing stroboscope apparatus.



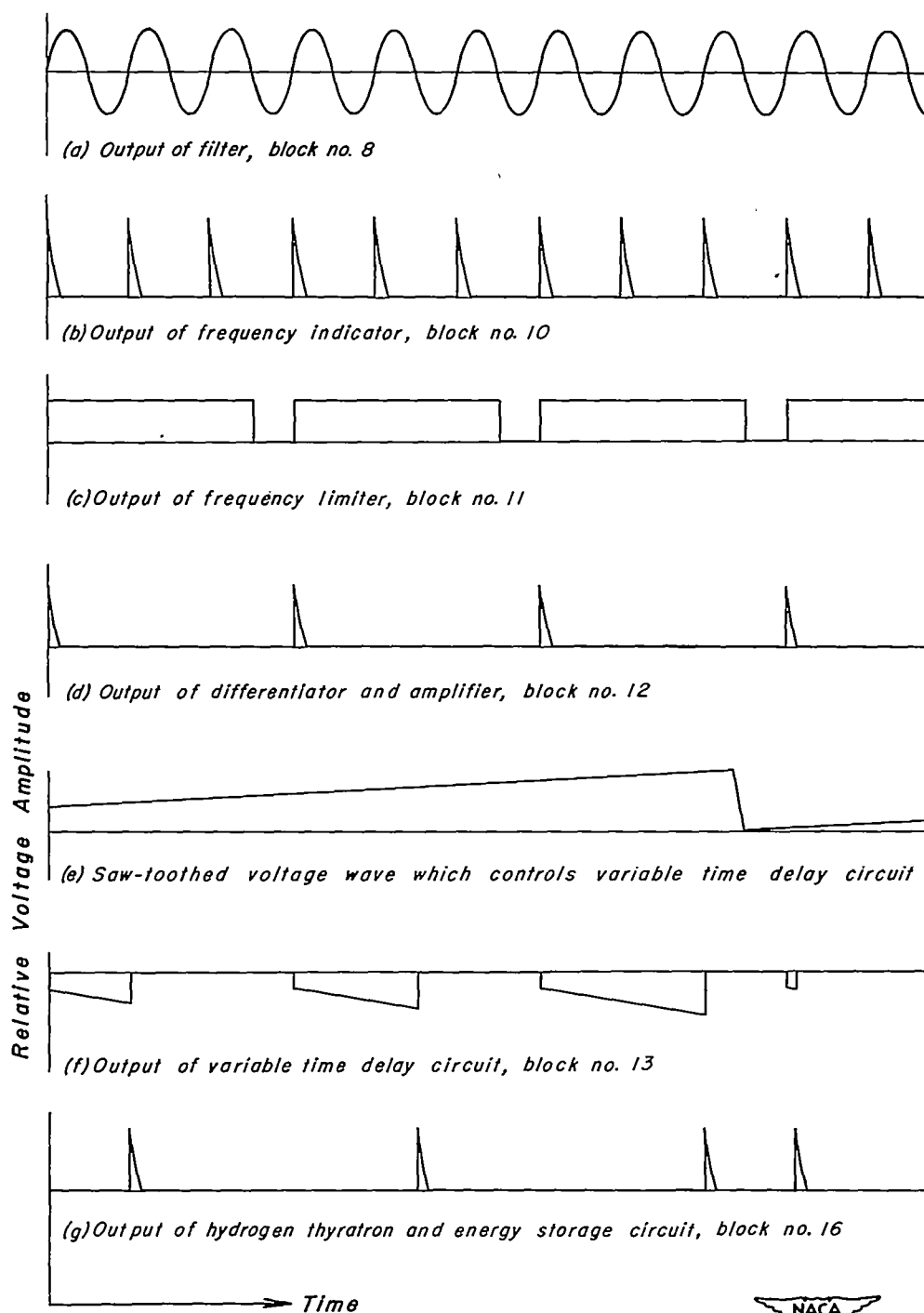
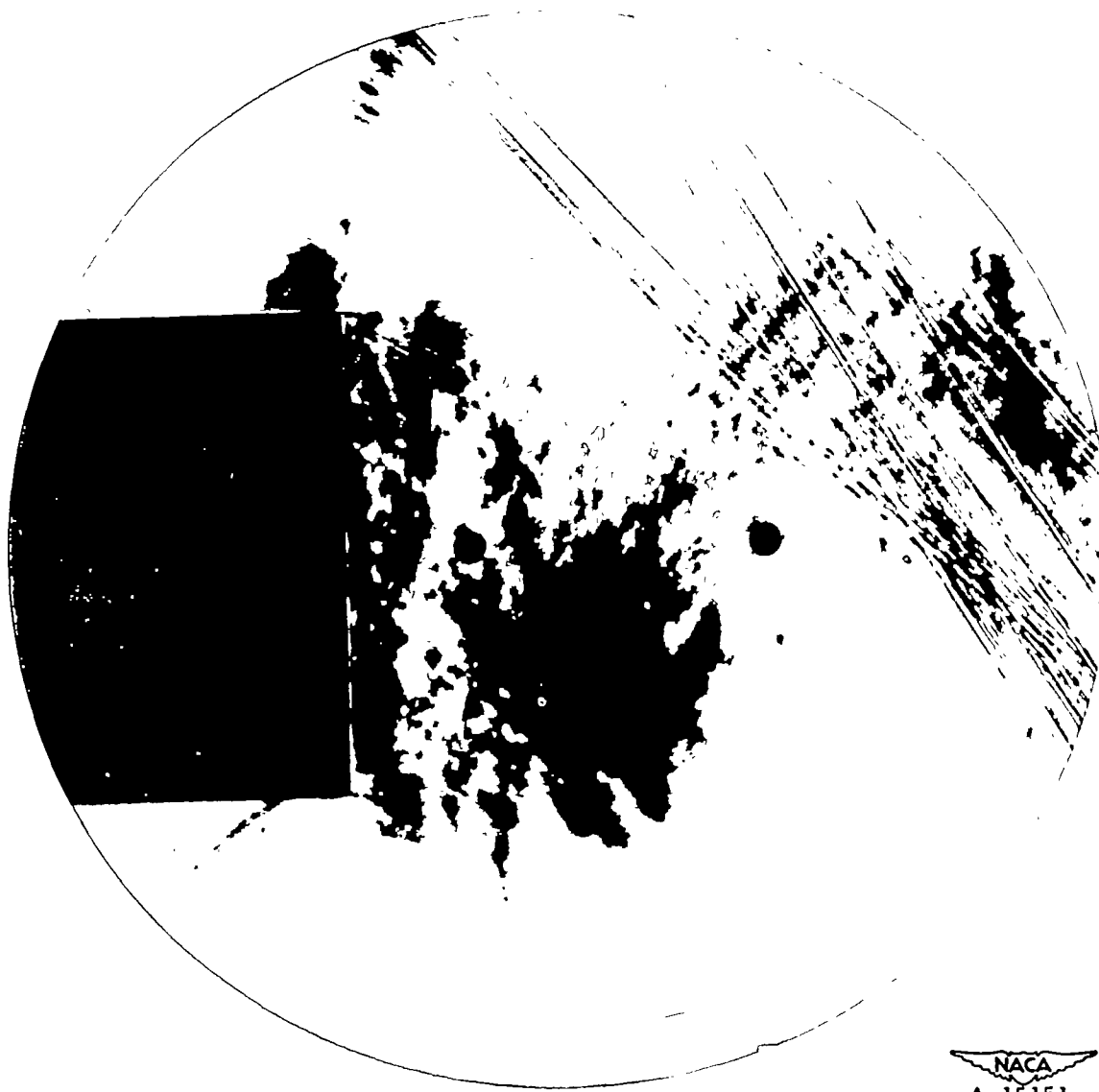


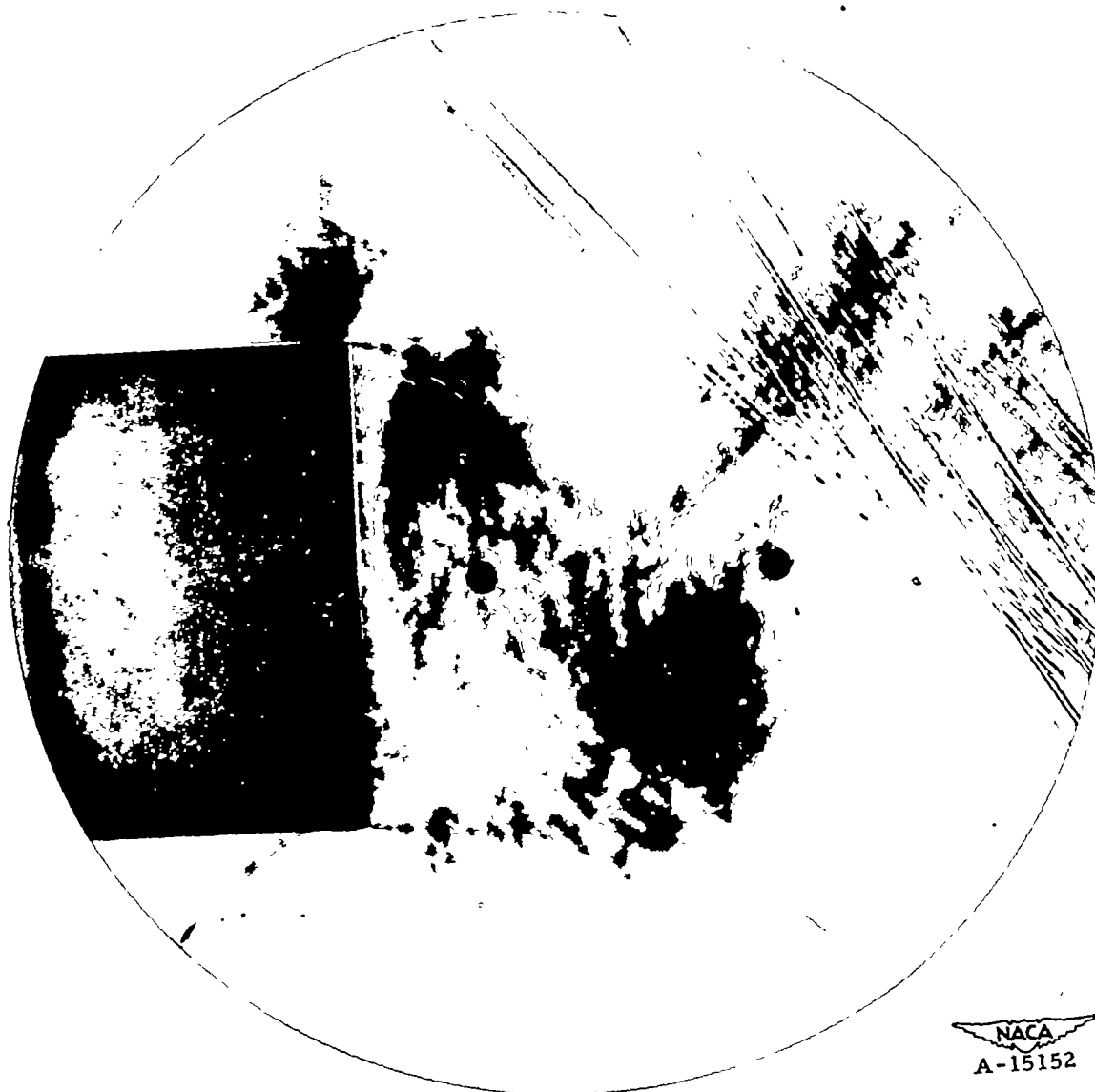
Figure 3.—Representative wave forms at various locations  
in the electronic circuit



NACA  
A-15151

(a) Boundary layer leaving upper surface of airfoil rolls up to start new vortex.

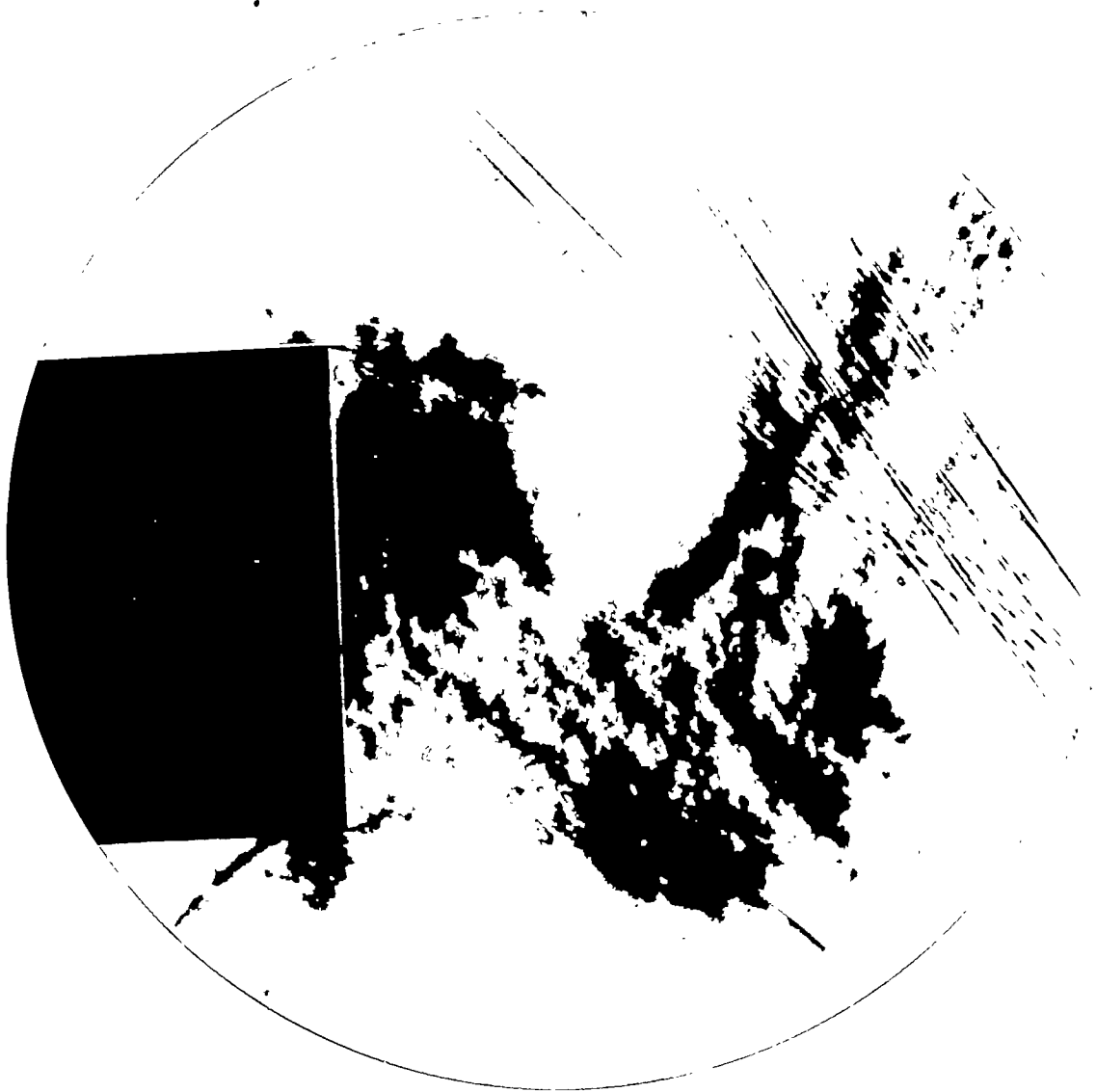
Figure 4.- Vortex discharge from the rear of a blunt trailing-edge airfoil. Discharge frequency, 150 cycles per second.



NACA  
A-15152

(b) Vortex forming off upper surface has attained approximately one-fourth ultimate size.

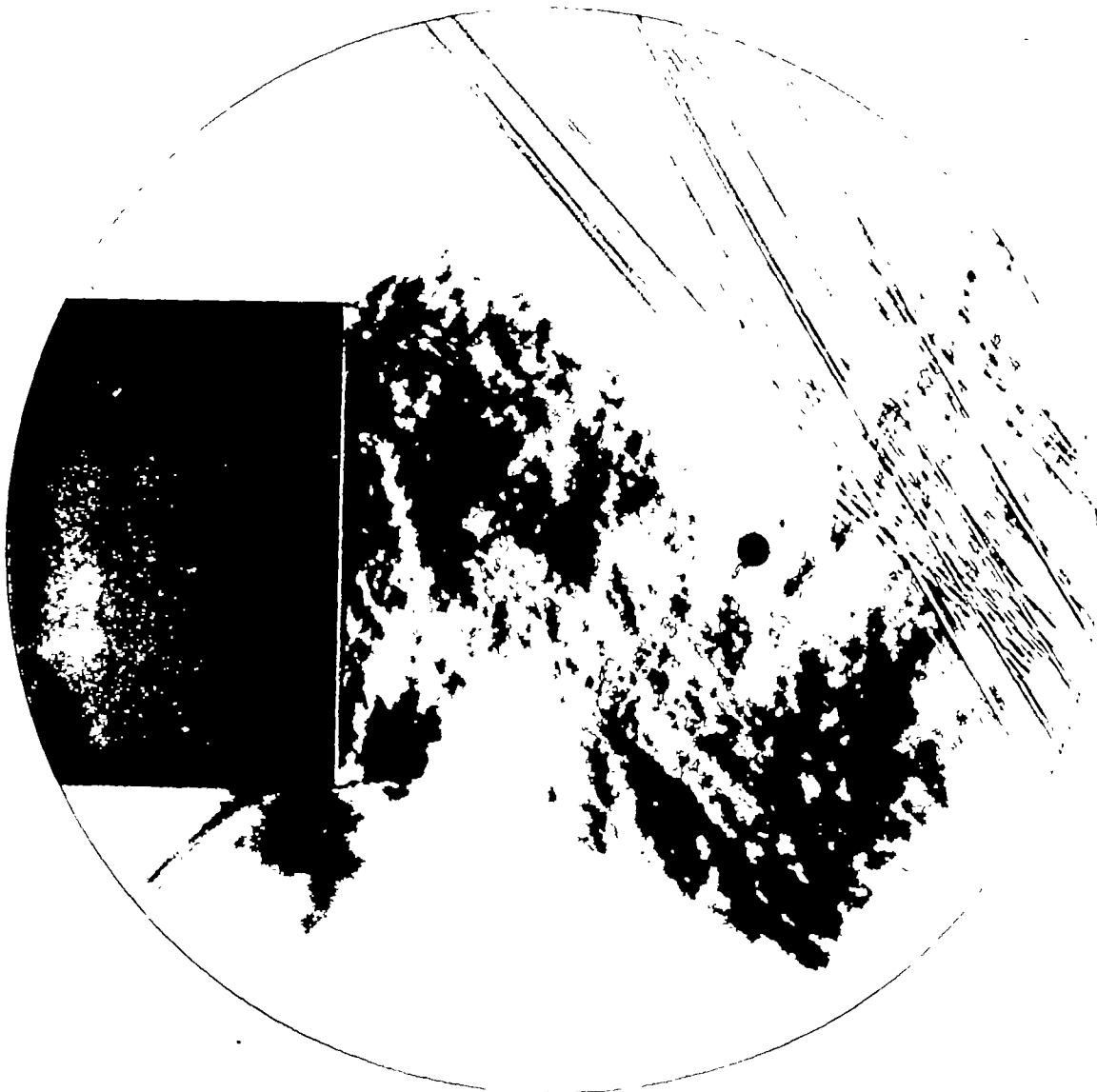
Figure 4.— Continued.



NACA  
A-15153

(c) Vortex from lower surface has become detached from the rear of the blunt trailing-edge airfoil.

Figure 4.- Continued.



NACA  
A-15154

(d) Vortex forming off upper surface approaches ultimate size.

Figure 4.— Continued.



NACA  
A-15155

(e) Vortex forming off upper surface immediately prior to detachment.

Figure 4.— Continued.



NACA  
A-15150

(f) Fully developed vortex from upper surface follows predecessor downstream.

Figure 4.- Concluded.





NACA  
A-15158

Figure 5.— Vortex discharge from rear of 1.770-inch-diameter cylinder. Discharge frequency, 450 cycles per second.



NACA  
A-15157

Figure 6.— Vortex discharge from rear of 0.590-inch-diameter cylinder. Discharge frequency, 2630 cycles per second.



Figure 7.— Vortex discharge from rear of 0.250-inch-diameter cylinder. Discharge frequency, 6250 cycles per second.



NACA  
A-15159

Figure 8.— Vortex discharge from rear of blunt trailing-edge airfoil. Discharge frequency, 6800 cycles per second.



Figure 9.— Vortex discharge from rear of blunt trailing-edge airfoil. Discharge frequency, 9520 cycles per second.

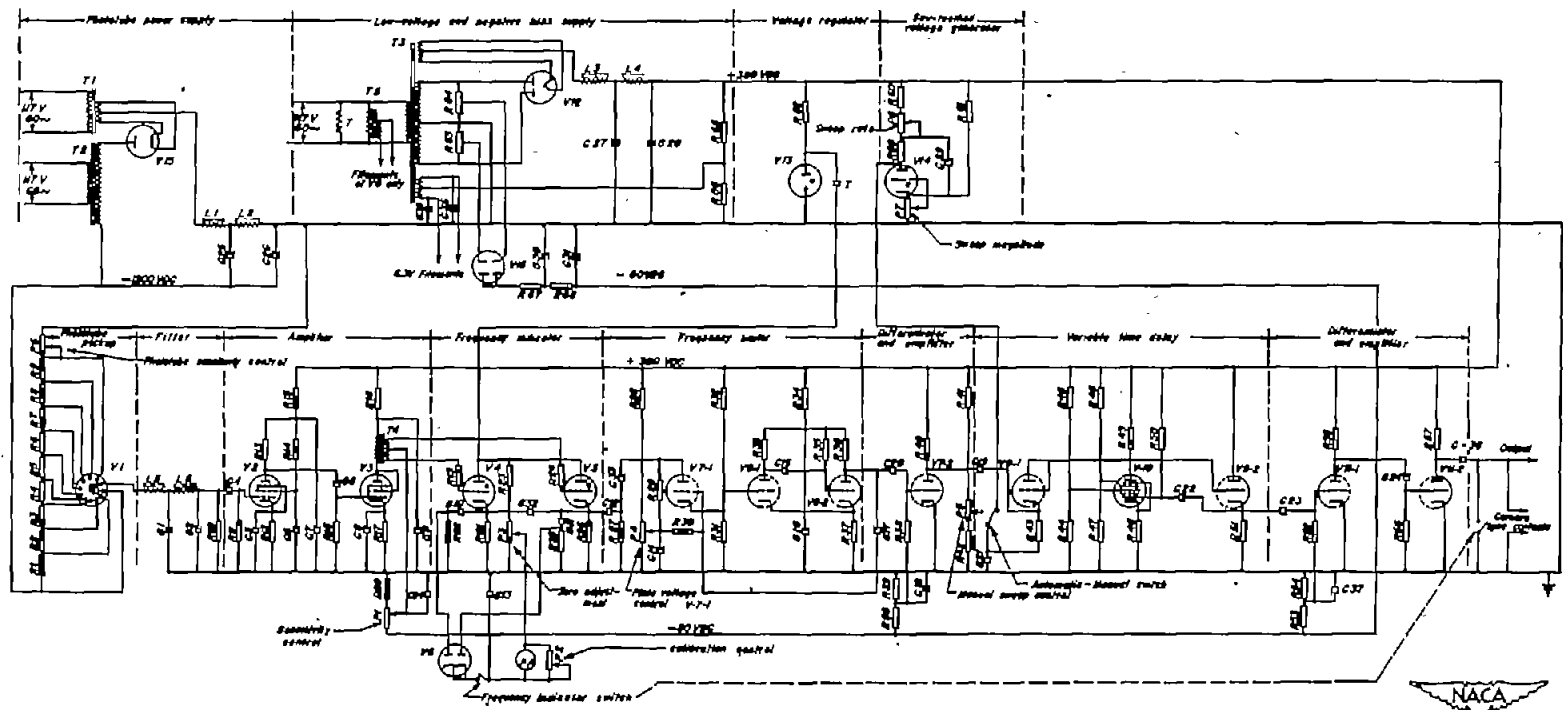


Figure 10.— Schematic drawing of self-synchronizing stroboscopic schlieren control circuits.

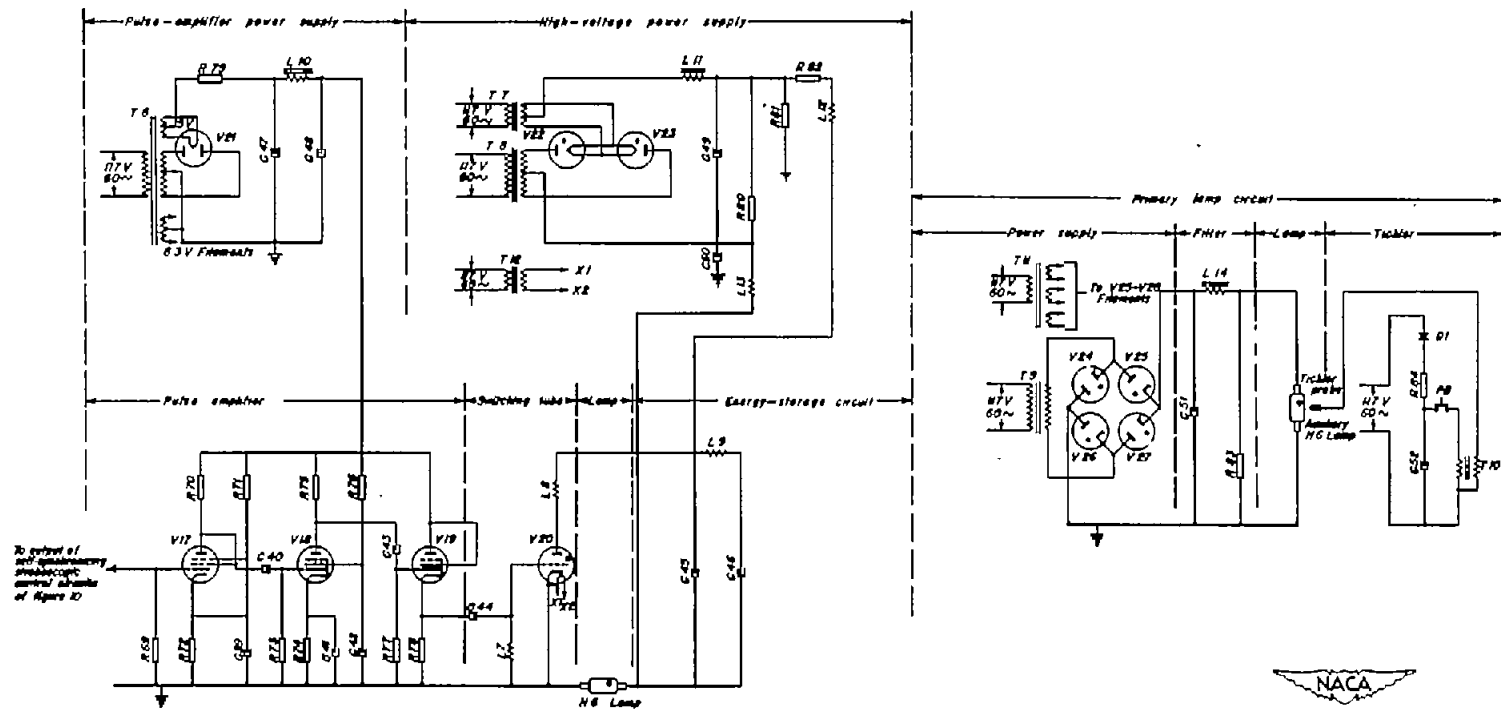


Figure 11.—Schematic drawing of self-synchronizing stroboscopic schlieren power circuits.